Environment, Development and Sustainability (2020) 22:1897–1911
https://doi.org/10.1007/s10668-018-0269-x

Experimental and CFD analysis to study the effect of inlet area ratio in a natural draft biomass cookstove

Rohan R. Pande[1] · **Milind P. Kshirsagar**[2] · **Vilas R. Kalamkar**[1]

Received: 16 November 2017 / Accepted: 8 October 2018 / Published online: 12 October 2018

Abstract

The biomass cookstoves have been used in rural areas for the time immemorial. New developments in cookstove design are needed due to cookstoves impact on the user's health and the environment. This paper presents a novel computational method to understand the working of a cookstove. The effect of inlet area ratio on various performance parameters is studied through experimentation and computational fluid dynamics (CFD). The steady-state model predicts the temperature profile at different locations inside the stove for different inlet area ratios (IARs), which is validated against the experimental data. The combustion phenomenon is simulated using non-premixed combustion and k-ε turbulence models. The critical value of IAR is found to be 0.70, up to which the firepower and flame temperature are increasing. For IAR less than 0.7, the firepower decreases, flame temperature saturates, and the CO emissions continue to rise. Results showed that CFD is a useful tool with adequate accuracy to understand the thermal and emissions behaviour of the cookstove. CFD can be used as an aid to the experimentation for preliminary analysis or as a standalone tool once validated experimentally.

Keywords CFD · Combustion · Biomass cookstove · k-ε turbulence model · Inlet area ratio · Non-premixed combustion

List of symbols

A_i	Cross-sectional area unoccupied by the fuel at the feed door, m^2
A	Cross-sectional area of elbow, m^2
T_{fg1}	Flue gas temperature in the combustion chamber, K
t_{avg}	Average time taken, s
$\dot{m}_{fuel}$	Mass flowrate of fuel, kg/s
h	Height of the stove, m
Q_{in}	Heat release by flue in combustion chamber, kW
$\dot{m}_{flue}$	Mass flowrate of flue, kg/s
C_p	Specific heat capacity of fuel, kJ/kgK

✉ Vilas R. Kalamkar
vilas.kalamkar@rediffmail.com

[1] Department of Mechanical Engineering, Visvesvaraya National Institute of Technology, Nagpur 440010, India

[2] St.Vincent Pallotti Engineering College, Nagpur, India

PM Particulate matter
CO Carbon monoxide

1 Introduction

The energy depletion can bring a threat to the functioning of the entire economy, particularly in developing economies (Bhowte 2016). India's substantial and sustained economic growth is placing an enormous demand on its energy resources. Biomass is one such major resource of energy, which has been used for since millennia for meeting myriad human needs, including energy. Main sources of biomass energy are trees, crops, and animal waste, which contribute over a third of the primary energy in India (Chouhan et al. 2014). According to the report of the national council for applied economic research (NCAER), biomass fuels contributed 90% of the energy in the rural areas and over 40% in the cities. Wood fuels, which contribute 56 percentage of total biomass energy (Sinha et al. 1994), are predominantly used in rural households for cooking, water and home heating, as well as by traditional and artisan industries (Jana and Bhattacharya 2017). Nowadays, the emphasis of biomass cookstove research is on improving the efficiency as well as emissions performance of the stoves. The global alliance for clean cookstoves with its 1800 + partner organizations from different sectors is working to increase global access to clean cookstoves and fuels. The alliance goal is to enable 100 million households to adopt clean cookstoves and fuels by 2020. The main aims of alliance partner organizations are to increase the efficiency, reduce indoor air pollution, and to develop reliable, clean, and affordable stoves so that people could benefit from them (Ting et al. 2012). Around 40% of the world population, mostly in developing countries, still uses traditional biomass as observed by the International Energy Agency (World Energy Outlook 2015). However, severe health issues are also associated with its use. Around 3–4 million people prematurely die every year, and many more are affected by morbidity due to indoor air pollution (IAP). Majority of the deaths occur amongst the person handling the cookstove; hence, awareness programs regarding the adverse effect of IAP should be conducted (Poddar and Chakrabarti 2016). The root cause for IAP is the exhaust coming out of the traditional biomass stoves. The incomplete combustion in stove leads to health-damaging products like carbon monoxide, particulate matter, which causes chronic obstructive lung disease, respiratory infections, and many more fatal diseases (WHO, Household air pollution and health 2018). Hence, to overcome such problems, major steps should be taken to redesign the traditional cookstoves or to develop new ones. A wide variety of cookstoves is available with varying performance (Kshirsagar and Kalamkar 2014; Manoj Kumar et al. 2013; Mehetre et al. 2017; Sutar et al. 2015). Many researchers from different parts of world have compared the emissions (PM and CO) from the traditional biomass cookstoves with the improved stoves (Grabow et al. 2013; Ludwinski et al. 2011; MacCarty et al. 2010; Pande et al. 2018; Singh et al. 2012, 2014).

Computational fluid dynamics (CFD) has become a powerful tool for the pure and applied research applications, and it focuses on the investigations of systems involving fluid flow, heat and mass transfer, combustion and other associated phenomena such as the study of chemical reactions through simulations. CFD may provide more detailed analysis in less time and cost than a physical model alone, but experimental validation of the CFD model is required. Ministry of New and Renewable Energy, Government of India, also recommended the CFD models for stove development work (Ministry of New and

Renewable Energy 2010). In a natural draft biomass stove, the fluid flow mechanism is caused due to the temperature difference in the combustion zone/chimney. Therefore, the development of the computational model for cookstove involves buoyancy, heat transfer, combustion, and chemical species reaction. The governing equations for CFD in the cookstove are conservation of energy, conservation of momentum, and chemical reactions. CFD simulation needs to be validated with the experimental results, and it can be predictive and reduce the physical prototyping and testing efforts. CFD includes two different models for solving combustion: one is premixed and the other as a non-premixed combustion model. In the last few years, some of the stove researchers started using CFD in design and analysing the cookstove (Dastoori et al. 2013; Weerasinghe and Bandara 2003; Varunkumar et al. 2012; Wohlgemuth et al. 2009). CFD is also used and proposed by a number of independent researchers for the design analysis and optimization of biomass stoves (Misra 2009; Ravi et al. 2002). In his thesis work, (Miller-Lionberg 2011) performed fine resolution CFD analysis using large eddy simulation (LES) technique for biomass cookstoves, giving a detailed literature review of the CFD applied to natural convection stoves. Some researchers, for the stove optimization purpose, uses genetic algorithms along with CFD (Bryden et al. 2003; Slipper et al. 2009).

The present work is a numerical simulation of the working of a natural convection rocket-type biomass cookstove, validated by the experiment conducted on the geometry proposed by Agenbroad et al. 2011. The effect of the parameter introduced by Kshirsagar and Kalamkar 2015, named inlet area ratio (IAR), has been investigated numerically and experimentally. The temperatures obtained by the computational method are validated with the experimental results. Further, the emissions predicted by the CFD simulation are also discussed in this paper.

2 Experimental set-up

An experimental set-up was designed and installed to conduct experiments on natural draft biomass cookstove as shown in Fig. 1a. The schematic sketch of the experimental set-up with the dimensions of the rocket biomass cookstove used for the work is as shown in Fig. 1b. The stove insulated with ceramic wool was kept on a calibrated weighing machine ranging from 0

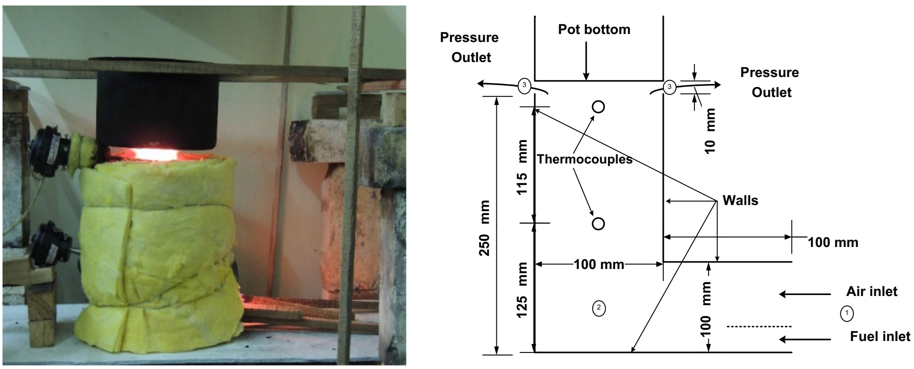

(a) (b)

Fig. 1 **a** Actual experimental set-up, **b** schematic sketch of the experimental set-up with boundary condition to 60 kg. Readings were noted down for the reduction of every 0.01 kg mass of fuel for 15 min from igniting. To separate out the mass of water evaporated from the mass of fuel burnt, the pot was kept hanging leaving a pot gap of 10 mm as shown in the actual experimental set-up. Nine sets of sticks with a constant cross section of 12 mm × 12 mm (relatively small in cross section as compared to typical wood used in the field) were experimented varying from 2 to 20 in number, resulting into IAR variation of 0.63–0.96. The extended elbow of the stove is used to feed the fuel, and no fuel shelf (grate) was used for experimentation. The term IAR was defined as per the Kshirsagar and Kalamkar 2015:

$$\mathrm{IAR}\left(A_r\right) = \frac{A_i}{A} = \frac{\text{Area unocuppied by the fuel at the feed door}}{\text{Cross-sectional area of the elbow diameter}} \quad (1)$$

The schematic representation of IAR is as shown in Fig. 2. Two *R*-type thermocouples were used to measure the flame temperature inside the chimney. The position of thermocouples is as shown in Fig. 1b.

2.1 Data reduction

The values of mass flow rates are determined through experimentation and are used as input conditions for computational work.

2.1.1 Mass burn rate of fuel

The mass burn rate of fuel was calculated by keeping the stove on the weighing machine. Time for every 0.01 kg fuel reduction was noted down for every set of IAR, from which an average time for a set of readings (t_{avg}) was calculated. The mass burn rate of fuel was calculated as:

$$\dot{m}_{\mathrm{fuel}} = \frac{0.01}{t_{\mathrm{avg}}} \quad (2)$$

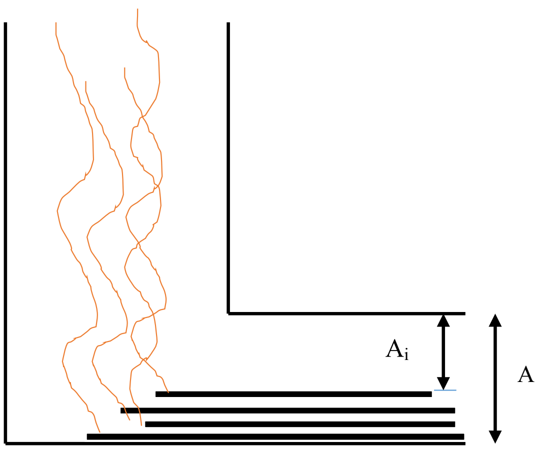

Fig. 2 Schematic representation of inlet area ratio, IAR

2.1.2 Mass flow rate of flue gas

In cookstove, heat is produced in the combustion chamber, and hence the chamber is considered as the control volume. Let temperatures be T_1 and T_2 at point 1 and 2 and the amount of heat released assuming all the heat goes into the flue gas, and neglecting heat losses through conduction and radiation is as shown in Eq. (3).

$$Q_{\text{in}} = m_{\text{flue}} C_p \left(T_1 - T_2\right) \tag{3}$$

As the density decreases due to the temperature variation in combustion chamber, a small pressure draught is created. The net change in pressure across the points 1 and 3, shown in Fig. 1b, is calculated by hydrostatic law as in Eq. (4).

$$\Delta P = gh\left(\rho_1 - \rho_3\right) \tag{4}$$

Applying Bernoulli's equation between point 1 and point 3,

$$gh\left(\rho_1 - \rho_3\right) = \frac{1}{2}\rho_1 v_1^2 \tag{5}$$

From the above equation, we get the velocity of flue gas through the chimney.

$$v_1 = \sqrt{2gh\left(\frac{\rho_1 - \rho_3}{\rho_1}\right)} \tag{6}$$

Theoretical mass of flue gas can be calculate as,

$$\dot{m}_{\text{flue}} = \rho_1 A v_1 \tag{7}$$

The mass flow rate of air required as a boundary condition to the CFD simulation is calculated from the correlation developed for the actual mass flow rate of flue gas through the same geometry by Kshirsagar and Kalamkar (2015). Kshirsagar and Kalamkar (2015) fits the linear equation to the experimental results from Agenbroad et al. (2011) as given below:

$$\dot{m}_{\text{flue}} = 0.012 * A_r - 0.006 \tag{8}$$

The mass flow rate of air is calculated as:

$$\dot{m}_{\text{air}} = \dot{m}_{\text{flue}} - \dot{m}_{\text{fuel}} \tag{9}$$

3 Computational model

The assumptions considered in the present simulation are as follows:

1. Though the operation of the cookstove is not at steady state, the average parameters over a period are more important than the instantaneous values. Therefore, the average performance of cookstove is assumed to be at a steady state (Baldwin 1987; Bhandari et al. 1988; Bussmann et al. 1983; Shah and Date 2011; Slipper et al. 2009).
2. A two-dimensional (2-D) FLUENT model is used to save the computational time (Bussmann et al. 1983; Chaney et al. 2012; Gupta and Mittal 2010; Ravi et al. 2002).

3. Since the inner wall and flame temperatures in the combustion zone hardly have any temperature difference (Agenbroad et al. 2011; Kshirsagar and Kalamkar 2015), the radiation heat exchange between the flame and the chamber wall is neglected.
4. The exhaust generated in the domain does not undergo any further chemical change.

ICEM and ANSYS FLUENT 14.5 were used for the geometry creation and simulation of the cookstove, respectively. The 2-D computational domain of the natural convection rocket-type cookstove is shown in Fig. 1b. The air and fuel input to the stove goes through the elbow diameter. The structured mesh was created using ICEM. FLUENT was then used to solve the parameters of the model. For the non-premixed combustion model, probability density function (PDF) was determined by using the ultimate and proximate analysis values of the biomass fuel used.

3.1 Grid independence test

Grid generation is the most important task before performing any CFD simulation. Adequately fine grids are generated to ensure the accurate flow computations. The grid independence test has been carried out initially for one case. The number of nodes was varied from 16,195 to 70,455. The values of temperature at point T_{fg1} in the stove for 65,349 and 70,455 nodes were having the difference of $< 1\%$, so the simulation was carried out with 65,349 nodes. In the similar fashion, the meshing was done for the other cases of the fluid domain before carrying out the simulation. The grid independence test values are shown in Table 1.

3.2 Governing equations

Since there is no premixing of fuel and air in the combustion chamber, non-premixed combustion model was used in FLUENT. Three fundamental equations, namely continuity equation, momentum equation, and energy equation, were solved in the model. In non-premixed combustion, PDF of the mixture fraction is selected for modelling the sub-grid scale mixing. The transport equation for conserved scalar mixture fraction is taken from Biswas and Eswaran (2002).

Table 1 Grid independence test for single pot

Sr.no.	No. of element	T_{fg1}	% difference
1.	16,195	840	–
2.	25,443	818	2.62
3.	49,901	787	3.78
4.	57,663	760	3.43
5.	61,535	756	0.52
6.	65,349	752	0.53
7.	70,455	751	0.13

3.3 Boundary conditions

In CFD analysis, it is very important to take proper initial and boundary conditions approximate to experimental values, to get appropriate results. The same inlet area ratios as that of the conducted experiment were used as the initial boundary condition for the CFD analysis. The results of the temperature profile in the combustion chamber were validated with the experimental values. Figure 1b shows the wall boundary conditions used.

3.3.1 Inlet

The elbow diameter of an inlet is 100 mm and was divided into two inlet boundary conditions. The division was done based on inlet area ratios obtained from the experiment. The mass flow rate of air and fuel mass burning rate were taken as two inlet boundary conditions as shown in Table 2. These mass flow rate values were obtained from experimental measurements. The temperature of air and fuel inlet was taken as 300 K. Also, turbulence intensity and turbulence viscosity ratio for inlet was taken as 5 and 10%, respectively (Fluent 2011). The turbulence intensity (I) is defined as the ratio of the root mean square of the velocity fluctuations, to the mean free stream velocity. The value of I for internal flow varies from 1 to 10%.

3.3.2 Outlet

Outlet boundary condition was specified in terms of atmospheric pressure (zero gauge pressure).

3.3.3 Wall

Wall boundary conditions are used to bound fluid and solid regions. In viscous flows, the no-slip boundary condition is enforced at walls by default, but we can specify a tangential velocity component in terms of the translational or rotational motion of the wall boundary, or model a slip wall by specifying shear. The pot bottom was also treated as a wall at 100 °C. The ultimate and proximate analysis of the wood is entered into the "coal calculator", which is a tab under non-premixed combustion model in FLUENT software, which

Table 2 Inlet boundary condition

Inlet area ratio	Fuel burning rate (kg/min)	Air mass flow (kg/min)
0.963	0.0045	0.329
0.927	0.0072	0.300
0.890	0.0090	0.272
0.835	0.0122	0.229
0.780	0.0156	0.186
0.743	0.0180	0.157
0.707	0.0216	0.127
0.670	0.0171	0.105
0.633	0.0152	0.081

Table 3 Proximate and ultimate analysis of fuel

Proximate analysis (%)		Ultimate analysis (%)	
Volatile matter	79	Carbon	49.98
Fixed carbon	11	Oxygen	43.84
Moisture	9	Hydrogen	6.02
Ash	1	Nitrogen	0.15
HHV	19000 kJ/kg	Sulphur	0.01

Table 4 Validation results

	Experimental values		Computational values		% error (top)	% error (middle)
IAR	Top (K)	Middle (K)	Top (K)	Middle (K)		
0.96	567	678	534	664	6	2
0.92	779	869	665	830	15	5
0.89	959	995	824	925	14	7
0.84	1045	1089	1165	1195	− 11	− 10
0.78	1071	1108	1082	1200	− 1	− 8
0.74	1075	1118	1204	1258	− 12	− 13
0.71	1076	1122	1130	1079	− 5	4
0.67	1079	1123	1173	1118	− 9	0.4
0.63	1081	1126	1108	1128	− 2	− 0.1

allows the user to enter the properties of fuel used (by default the values are given for coal and hence named as "Coal Calculator"). The values are shown in Table 3.

4 Results and discussion

Computational values were validated by comparing with the experimental values for the same geometrical and operational parameters. The experimental dataset included nine different IAR values (0.63–0.96). The temperature in the combustion chamber for the experimental and computational trials at different IARs is given in Table 4. The simulation values showed a good agreement with the experimental values. The average deviation in the CFD and experimental results is 4.6%, which is quite low and acceptable. This shows the accuracy and effectiveness of the CFD tool in solving such problems. Hence, the other results obtained through computational method can be used to interpret the working of the cookstove.

4.1 Effect on flame temperatures

Table 4 shows the variation of flame temperature with different IAR values. The flame temperature increases with decreasing the IAR. Figure 3 shows the complete temperature contours obtained inside the stove body from the simulation for different IARs. It is observed that below IAR = 0.71 value, the flame temperatures showed hardly any change.

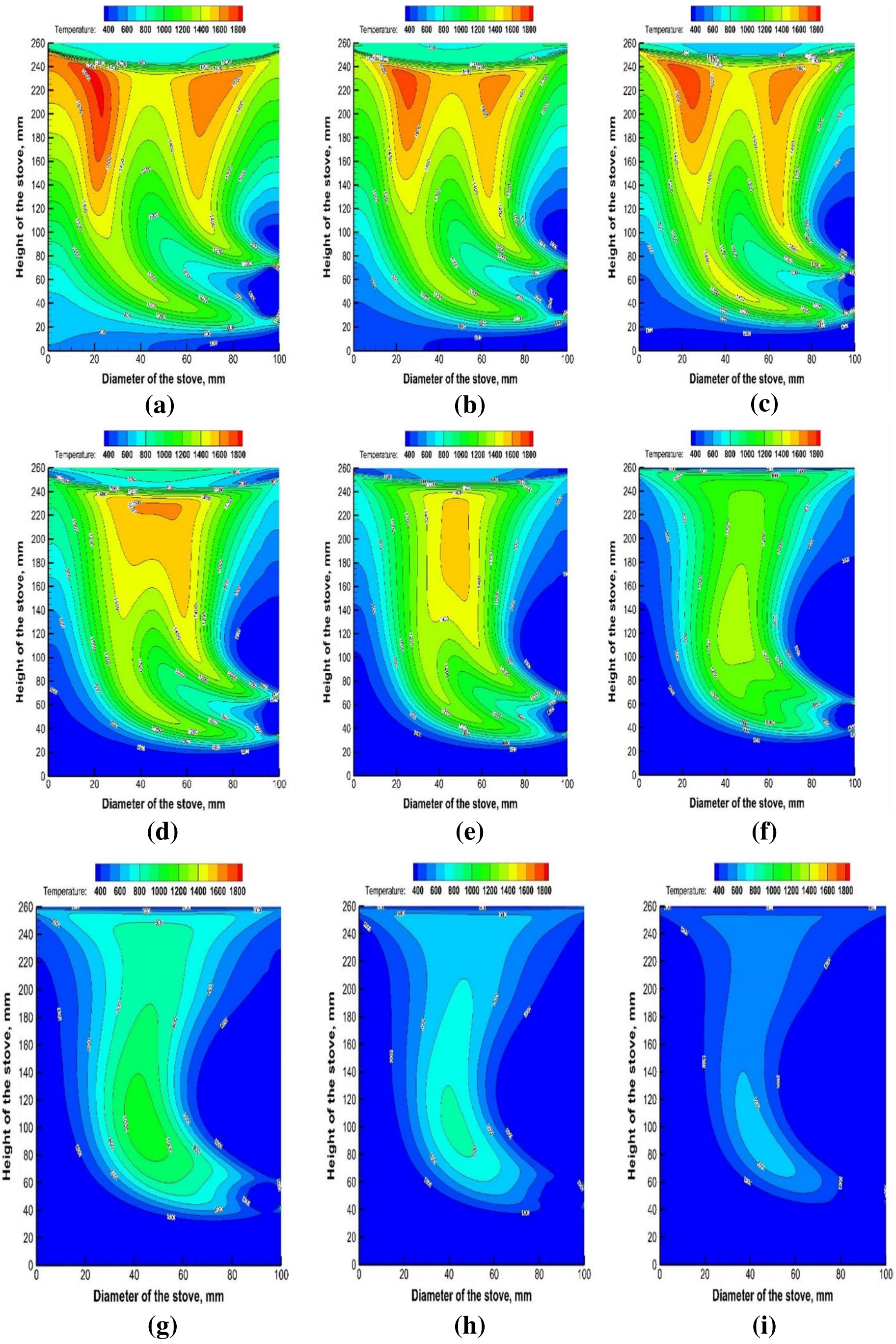

Fig. 3 Temperature contours for different inlet area ratios, (IARs). **a** 0.63, **b** 0.67, **c** 0.71, **d** 0.74, **e** 0.78, **f** 0.84, **g** 0.89, **h** 0.92, **i** 0.96

This is due to the decrease in the available air for the combustion with lower values of IAR. As we further decrease the IAR by increasing the number of sticks, the firepower increases to maximum and then starts decreasing afterwards. The variation of firepower with flame temperature follows the same trend obtained in the literature (Agenbroad et al. 2011; Kshirsagar and Kalamkar 2015).The variation of flame temperature with the height is also visible in Fig. 3.

4.2 Effect of IAR on firepower (FP)

The value of IAR drops with the increasing number of sticks fed to the stove. Figure 4 shows that with the decrease in the value of IAR, the firepower increases up to a certain point, which can be called as a choking point of the stove and corresponds to the critical inlet area ratio. It can be seen that the firepower at critical inlet area ratio is maximum. It can be seen that the critical inlet area ratio here predicted by CFD simulation is 0.7, which is nearly equal to that predicted by Kshirsagar and Kalamkar 2015 using algebraic heat and mass transfer model.

4.3 Effect on the CO concentration

For higher values of IAR, the amount of air entering the stove is more and hence the concentration of CO molecules decreases partly because of additional dilution air and availability of abundant oxygen for complete combustion as shown in Fig. 5. However, as the IAR goes on reducing, the CO concentration goes on increasing, due to the lesser availability of combustion air and less dilution. The temperatures obtained both by experimental

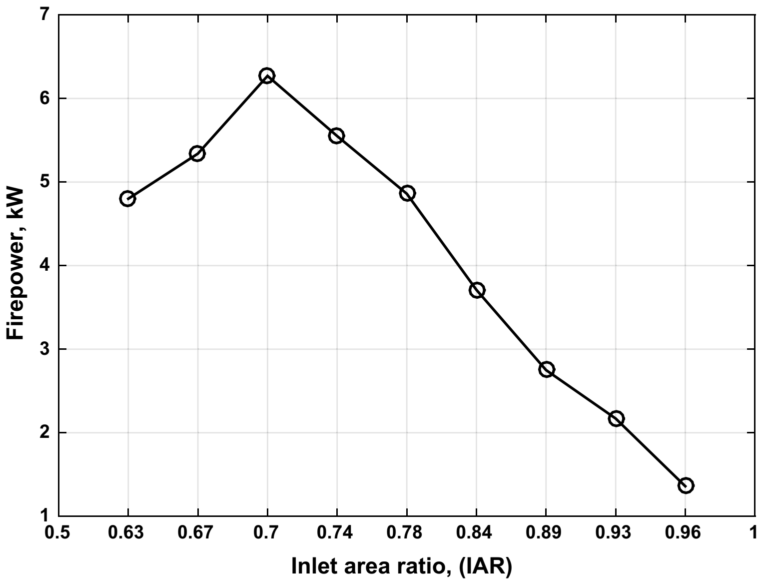

Fig. 4 Variation of firepower with IAR

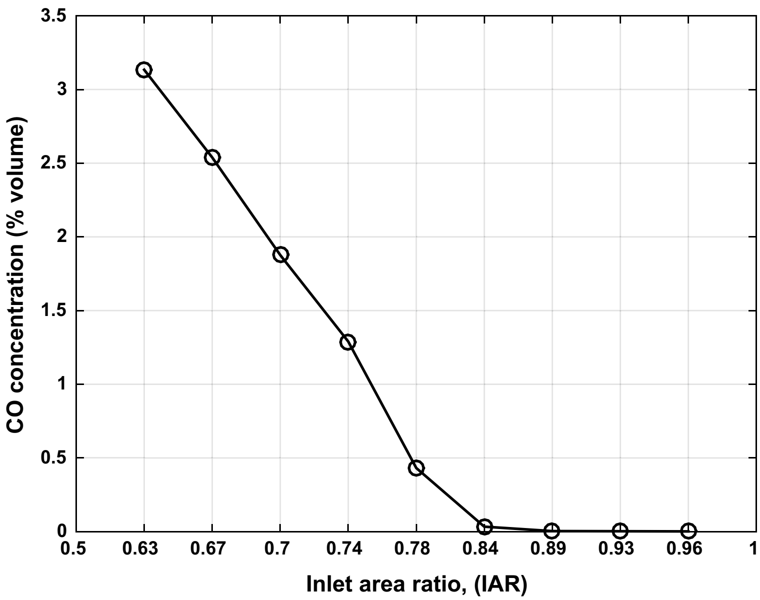

Fig. 5 Variation of CO concentrations with the inlet area ratio, IAR

and computational showed that there is hardly any change in the values of temperature for less than 0.7 IAR.

4.4 Effect on the CO_2 concentration

The variation of CO_2 with IAR is as shown in Fig. 6. It shows a similar trend like the variation of firepower with IAR in Fig. 4. This is understandable as the CO_2 content of a flue gas is a direct representation of its firepower. However, one can notice the rise in firepower with decreasing IAR is almost linear up to IAR = 0.7 in Fig. 4. This is due to the decrease in combustion efficiency with decreasing IAR and hence the conversion of fuel to CO_2. Also, less air provides less dilution, so concentration in the flue gas decreases.

4.5 Effect on the combustion efficiency

Initially, at higher values of IAR, the amount of air entering into the combustion chamber is high. It leads to a complete mixing of air and fuel which causes the rise in the combustion efficiency. It can be observed from Fig. 7 that for very low values of IAR the modified combustion efficiency (MCE) drops down.

The MCE can be calculated as,

$$\text{MCE}, \eta_C = \frac{\text{CO}_2}{\text{CO}_2 + \text{CO}}$$

As already discussed above, the value of CO is very low for higher values of IAR leading to higher MCE. Table 5 shows the model-predicted composition of exhaust in the cookstove for different IAR and firepower.

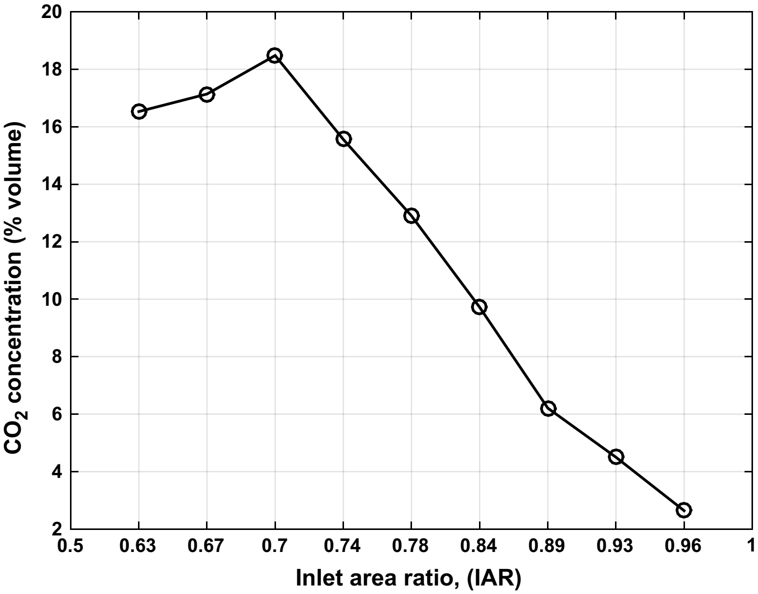

Fig. 6 Variation of CO_2 concentrations with inlet area ratio, IAR

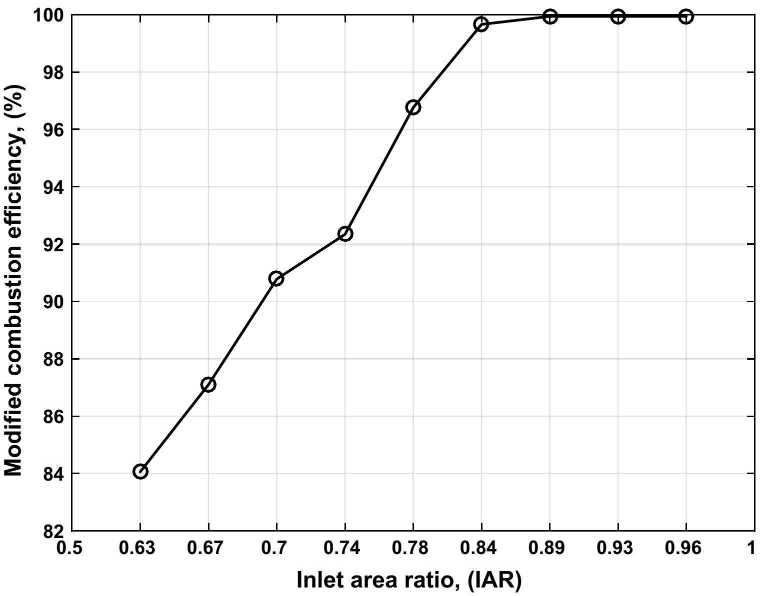

Fig. 7 Variation of modified combustion efficiency with IAR

Table 5 Model-predicted gas composition for varying IAR and firepower

FP	IAR	CO	CO_2	O_2	CO/CO_2	CO emission factor	CO indoor emissions	η_c
(kW)	–	(%)	(%)	(%)	–	(g/kg of fuel)	(g/min)	(%)
1.36	0.96	0.002	2.64	19.5	0.00061	0.08	0.0001	99.9
2.17	0.92	0.003	4.50	19.3	0.00058	0.11	0.001	99.8
2.75	0.89	0.004	6.21	17.8	0.00056	0.12	0.001	99.7
3.71	0.84	0.034	9.72	14.7	0.00345	0.85	0.01	99.7
4.86	0.78	0.432	12.9	11.6	0.03347	8.58	0.19	96.8
5.55	0.74	1.290	15.6	8.80	0.08290	22.18	0.65	92.3
6.27	0.71	1.877	18.5	5.39	0.10157	26.33	1.04	90.8
5.34	0.67	2.539	17.1	5.02	0.14811	44.74	1.19	87.1
4.8	0.63	3.134	16.5	2.91	0.18964	60.04	1.28	84.1

5 Conclusion

The effect of IAR on the performance of a natural draft biomass cookstove was studied computationally and experimentally. Several major outcomes can be concluded from the present analysis:

1. The temperatures obtained with the computational model and the experimental trial showed good agreement; hence, CFD was demonstrated to be an effective tool for the thermal analysis of the cookstove evaluated in this study.
2. The IAR is a critical parameter for the performance of a natural convection direct combustion type of cookstove and affects all the important performance parameters such as firepower, flame temperatures and emissions. The critical value of IAR is found to be 0.70, up to which the firepower and flame temperature are increasing. For IAR less than 0.7, the firepower decreases, flame temperature saturates, and the CO emission continues to increase.
3. It can be concluded that the operational parameter, IAR, has a considerable effect on the performance of a natural convection direct combustion type of cookstove and, hence, should be considered while designing a cookstove.

Acknowledgements No external funds were provided by any institution.

Compliance with ethical standards

Conflicts of interest The authors declare that they have no conflicts of interest.

References

Agenbroad, J., DeFoort, M., Kirkpatrick, A., & Kreutzer, C. (2011). A simplified model for understanding natural convection driven biomass cooking stoves-Part 1: Setup and baseline validation. *Energy for Sustainable Development. International Energy Initiative*. https://doi.org/10.1016/j.esd.2011.04.004.

Baldwin, S. F. (1987). *Biomass stoves: Engineering design development and dissemination*. Arlington, VA: Vita Publications.
Bhandari, S., Gopi, S., & Date, A. (1988). Investigation of CTARA wood-burning stove. Part I. *Experimental Investigation. Sadhana, 13*(4), 271–293. https://doi.org/10.1007/BF02759889.
Bhowte, Y. W. (2016). Forecasting the load of demand and supply of electricity in India. In *2016 International Conference on Computation of Power, Energy, Information and Communication, ICCPEIC 2016*, pp. 675–679. https://doi.org/10.1109/iccpeic.2016.7557308.
Biswas, G., & Eswaran, V. (2002). *Turbulent flows-fundamentals, experiments and modeling* (2002nd ed.). United Kingdom: Alpha Science International Ltd.
Bryden, K. M., Ashlock, D. A., McCorkle, D. S., & Urban, G. L. (2003). Optimization of heat transfer utilizing graph based evolutionary algorithms. *International Journal of Heat and Fluid Flow, 24*(2), 267–277. https://doi.org/10.1016/S0142-727X(02)00243-6.
Bussmann, P. J. T., Visser, P., & Prasad, K. K. (1983). Open fires: Experiments and theory. *Proceedings of the Indian Academy of Sciences Section C: Engineering Sciences, 6*(1), 1–34. https://doi.org/10.1007/BF02843288.
Chaney, J., Liu, H., & Li, J. (2012). An overview of CFD modelling of small-scale fixed-bed biomass pellet boilers with preliminary results from a simplified approach. *Energy Conversion and Management, 63,* 149–156. https://doi.org/10.1016/j.enconman.2012.01.036.
Chouhan, K., Ladhe, Y., & Upadhayay, V. (2014). Biomass a versatile fuel for energy and power generation. *IOSR Journal of Mechanical and Civil Engineering*. http://www.iosrjournals.org/iosr-jmce/papers/ICAET-2014/me/volume-3/2.pdf.
Dastoori, K., Makin, B., Kolhe, M., Des-Roseaux, M., & Conneely, M. (2013). CFD modelling of flue gas particulates in a biomass fired stove with electrostatic precipitation. *Journal of Electrostatics, 71*(3), 351–356. https://doi.org/10.1016/j.elstat.2012.12.039.
Fluent. (2011). *ANSYS FLUENT user's guide.* Vol. 15317. http://cdlab2.fluid.tuwien.ac.at/LEHRE/TURB/Fluent.Inc/v140/flu_ug.pdf.
Grabow, K., Still, D., & Bentson, S. (2013). Test kitchen studies of indoor air pollution from biomass cookstoves. *Energy for Sustainable Development, 17*(5), 458–462. https://doi.org/10.1016/j.esd.2013.05.003.
Gupta, R., & Mittal, N. D. (2010). Fluid flow and heat transfer in a single-pan wood stove. *International Journal of Engineering Science, 2*(9), 4312–4324.
Jana, C., & Bhattacharya, S. C. (2017). Sustainable cooking energy options for rural poor people in India: an empirical study. *Environment, Development and Sustainability, 19*(3), 921–937. https://doi.org/10.1007/s10668-016-9774-y.
Kshirsagar, M. P., & Kalamkar, V. R. (2014). A comprehensive review on biomass cookstoves and a systematic approach for modern cookstove design. *Renewable and Sustainable Energy Reviews*. https://doi.org/10.1016/j.rser.2013.10.039.
Kshirsagar, M. P., & Kalamkar, V. R. (2015). *A mathematical tool for predicting thermal performance of natural draft biomass cookstoves and identification of a new operational parameter. Energy* (Vol. 93). Amsterdam: Elsevier Ltd. https://doi.org/10.1016/j.energy.2015.09.015.
Kumar, M., Kumar, S., & Tyagi, S. K. (2013). Design, development and technological advancement in the biomass cookstoves: A review. *Renewable and Sustainable Energy Reviews, 26,* 265–285. https://doi.org/10.1016/j.rser.2013.05.010.
Ludwinski, D., Moriarty, K., & Wydick, B. (2011). Environmental and health impacts from the introduction of improved wood stoves: Evidence from a field experiment in Guatemala. *Environment, Development and Sustainability, 13*(4), 657–676. https://doi.org/10.1007/s10668-011-9282-z.
MacCarty, N., Still, D., & Ogle, D. (2010). *Fuel use and emissions performance of fifty cooking stoves in the laboratory and related benchmarks of performance. Energy for sustainable development* (Vol. 14). Amsterdam: Elsevier Inc. https://doi.org/10.1016/j.esd.2010.06.002.
Mehetre, S. A., Panwar, N. L., Sharma, D., & Kumar, H. (2017). Improved biomass cookstoves for sustainable development: A review. *Renewable and Sustainable Energy Reviews*. https://doi.org/10.1016/j.rser.2017.01.150.
Miller-Lionberg, D. (2011). A fine resolution CFD simulation approach for biomass cook stove development. http://gradworks.umi.com/14/92/1492414.html.
Ministry of New and Renewable Energy, G. of I. (2010). *New initiative for development and deployment of improved cookstoves: Recommended action plan, Final Report*.
Misra, J. S. (2009). Considering value of information when using CFD in design. Graduate Theses and Dissertations. 11087 Ames Laboratory (AMES), Ames, IA (United States). https://lib.dr.iastate.edu/etd/11087/?utm_source=lib.dr.iastate.edu%2Fetd%2F11087%26utm_medium=PDF%26utm_campaign=PDFCoverPages. Accessed 12 Oct 2018.

Pande, R. R., Kalamkar, V. R., & Kshirsagar, M. (2018). Making the popular clean: improving the traditional multipot biomass cookstove in Maharashtra, India. *Environment, Development and Sustainability.*. https://doi.org/10.1007/s10668-018-0092-4.

Poddar, M., & Chakrabarti, S. (2016). Indoor air pollution and women's health in India: An exploratory analysis. *Environment, Development and Sustainability, 18*(3), 669–677. https://doi.org/10.1007/s10668-015-9670-x.

Ravi, M. R., Kohli, S., & Ray, A. (2002). Use of CFD simulation as a design tool for biomass stoves. *Energy for Sustainable Development, 6*(2), 20–27. https://doi.org/10.1016/S0973-0826(08)60309-9.

Shah, R., & Date, A. W. (2011). Steady-state thermochemical model of a wood-burning cook-stove. *Combustion Science and Technology, 183*(4), 321–346. https://doi.org/10.1080/00102202.2010.516617.

Singh, S., Gupta, G. P., Kumar, B., & Kulshrestha, U. C. (2014). Comparative study of indoor air pollution using traditional and improved cooking stoves in rural households of Northern India. *Energy for Sustainable Development, 19*(1), 1–6. https://doi.org/10.1016/j.esd.2014.01.007.

Singh, A., Tuladhar, B., Bajracharya, K., & Pillarisetti, A. (2012). Assessment of effectiveness of improved cook stoves in reducing indoor air pollution and improving health in Nepal. *Energy for Sustainable Development, 16*(4), 406–414. https://doi.org/10.1016/j.esd.2012.09.004.

Sinha, C. S., Venkata, R. P., & Joshi, V. (1994). Rural energy planning in India designing effective intervention strategies. *Energy Policy, 22,* 403–414.

Slipper, B.-, Nottingham, T., & User, N. E., Burnham-Slipper, H. (2009). Breeding a better stove : The use of computational fluid dynamics and genetic algorithms to optimise a wood burning stove for Eritrea. Ph.D. thesis, University of Nottingham.

Sutar, K. B., Kohli, S., Ravi, M. R., & Ray, A. (2015). Biomass cookstoves: A review of technical aspects. *Renewable and Sustainable Energy Reviews, 41,* 1128–1166. https://doi.org/10.1016/j.rser.2014.09.003.

Ting, Z., Shivakoti, G. P., Haiyun, C., & Maddox, D. (2012). A survey-based evaluation of community-based co-management of forest resources: A case study of Baishuijiang National Natural Reserve in China. *Environment, Development and Sustainability, 14*(2), 197–220. https://doi.org/10.1007/s10668-011-9316-6.

Varunkumar, S., Rajan, N. K. S., & Mukunda, H. S. (2012). Experimental and computational studies on a gasifier based stove. *Energy Conversion and Management, 53*(1), 135–141. https://doi.org/10.1016/j.enconman.2011.08.022.

Weerasinghe, W. M. S. R., & Bandara, R. M. P. S. (2003). Computational modelling of a wood fired semi-enclosed cooking stove. In *2nd International Conference on Heat Transfer, Fluid Mechanics and Thermodynamics, WW1*. Accessed 12 Oct 2018.

WHO, Household air pollution and health. (2018). http://www.who.int/en/news-room/fact-sheets/detail/household-air-pollution-and-health.

Wohlgemuth, A., Mazumder, S., & Andreatta, D. (2009). Computational heat transfer analysis of the effect of skirts on the performance of third-world cookstoves. *Journal of Thermal Science and Engineering Applications, 1*(4), 41001. https://doi.org/10.1115/1.4001483.

World Energy Outlook. (2015). https://www.iea.org/Textbase/npsum/WEO2015SUM.pdf. Accessed 22 April 2018.